6-15-2011

Solar to Electrical Conversion via Liquid Crystal Elastomers

T. Hiscock

M. Warner

Peter Palffy-Muhoray
Kent State University - Kent Campus, mpalffy@cpip.kent.edu

Solar to electrical conversion via liquid crystal elastomers

T. Hiscock,[1] M. Warner,[1,a)] and P. Palffy-Muhoray[2]
[1]*Cavendish Laboratory, University of Cambridge, 19 JJ Thomson Avenue, Cambridge CB3 0HE, United Kingdom*
[2]*Liquid Crystal Institute, Kent State University, Kent, Ohio 44242, USA*

(Received 16 November 2010; accepted 14 March 2011; published online 19 May 2011)

We have constructed a hypothetical charge pump which converts solar energy into DC electricity. The output is generated by cyclic changes in the capacitance of a circuit, which transfers charge from a low to a high voltage. The electric field across the capacitor must be of the order of $10^8 \mathrm{Vm}^{-1}$ to compete with efficiencies of photovoltaics. We have modeled the output using a liquid crystal elastomer as the working substance. Efficiencies of $1-4\%$ are obtained, and are enhanced by careful choices in the capacitor geometries and the operating voltages of the charge pump. [doi:10.1063/1.3581134]

I. INTRODUCTION

Science and technology play a vital role in developing solar power technologies. Silicon based photovoltaics attain efficiencies of 10%[1] and currently produce six GW electricity worldwide.[2] A competitive technology, steam generation, generates AC electricity via turbines, the heat coming from vast arrays of concentrating mirrors. Huge desert power plants, such as Nevada Solar One, can have efficiencies as large as 20%.[3]

A reversible cycle of solar heating and cooling can produce an electrical output limited, in theory, only by the high and low temperatures of the cycle. In this article, we propose such a device in the guise of a DC charge pump. A capacitor is heated at constant charge from a high to a low capacitance state. Accordingly, the potential across the capacitor must rise, and can finally transfer charge from a low to a high voltage. We will first consider a liquid-crystal filled capacitor of fixed geometry where the capacitance change comes purely from the reduction on heating of the component of the dielectric tensor along the field, especially if there is a phase transition in the temperature range of interest. They are anisotropic fluids with a temperature-dependent orientational order, and hence also dielectric tensor. Heating induces a transition from a highly ordered to an isotropic state. From a microscopic point of view, heating in an external electric field creates a higher energy state since the molecular dipoles are not so aligned with the field.

We shall also examine liquid crystal elastomers for use in the hypothetical charge pump. In addition to a variable dielectric tensor from the liquid crystallinity, they have an added coupling of strain to this nematic order, a property which elsewhere finds diverse technological applications, e.g., electroactuation, artificial muscles, microfluidics. Now there are two, simultaneous sources of capacitance change: the dielectric tensor changes, as above, but also if the elastomer is itself the capacitor (with flexible electrodes on each face) then the geometry of the capacitor is additionally changing with temperature. Additionally, since charges are not so mobile as in a bulk liquid, breakdown is delayed and higher operating voltages can be used.

We explore the suitability of these materials for a charge pump, and optimize their performance by designing an appropriate electrical circuit. We begin by discussing relevant background theory, specifically the charge pump circuitry and the properties of both liquid crystals and liquid crystal elastomers. We shall then outline the proposed cycle of heating and cooling which transfers charge to a higher voltage. A model for these changes is constructed and we compute, and optimize, the efficiency of the pump for a number of capacitor geometries. We end with a discussion of the central theme of this article: is our proposed charge pump an efficient, viable and effective way to harness solar energy?

II. BACKGROUND THEORY

A. Charge pumps

The circuit diagram of the charge pump is shown in Fig. 1. The main component of the circuit is the capacitor - the capacitance changes when heated. The arrangement of diodes mean charge can only flow from the low voltage, V_1, to the high voltage, V_2. Though the circuit of Fig. 1(a) is modeled, there are other possibilities. Figure 1(b) shows a more practical circuit which avoids depletion of the source battery, V_1. Next, we will examine the cycle of heating and cooling of the capacitor in some detail, as sketched in Fig. 2. Over a cycle, the charge pump produces a net work output W as charge is pumped to the higher voltage. This crucially relies on the capacitance decreasing upon heating.

Consider heating from the lowest temperature, T_N (state A). The capacitance decreases and the left diode prevents backflow of charge. $V_C = q/C$ implies the voltage across the capacitor increases as the capacitance decreases, and the diode means the capacitor is now electrically isolated. At T_B, the voltage is $V_C = V_2$ (state B) and further decreases in capacitance now cause the charge on the capacitor to decrease finally to $q_2 = C_I V_2$ (state C), since charge can now flow through the right diode. This means charge is pumped into V_2 at constant voltage.

a)Electronic mail: mw141@cam.ac.uk.

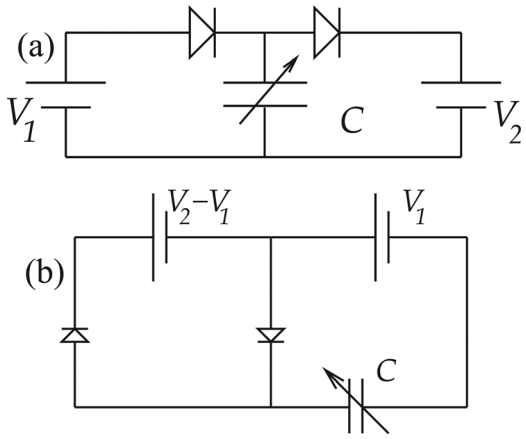

FIG. 1. (a) Charge pump: model circuit. Charge is pumped from the source V_1 to the higher voltage V_2. (b) A more practical circuit which recharges the source battery.

Upon cooling from the high temperature state, the reverse happens. Initially the capacitor increases from C_I to C_D and the voltage drops back to V_1 at constant charge. Then, as the capacitance further increases back to its initial value C_N, the battery V_1 charges the capacitor to its initial charge state q_1. The changes are considered adiabatic if they are slow compared to $t = RC$, where R is a characteristic circuit resistance. The output of this charge pump follows from: a total charge $q_1 - q_2$ is pumped into V_2 in stages B to C and the same charge, $q_1 - q_2$, is supplied by V_1 in stages D to A. Thus, the net work supplied per cycle is $W = (q_1 - q_2)(V_2 - V_1)$. To maximize this output, consider fixed high and low temperature states, with corresponding capacitances C_N and C_I - there is only freedom in choosing the intermediate state, C_B. There is a compromise between having C_B too large (not much charge is transferred) and having C_B too small (not enough of a voltage jump). More quantitatively, we can write $q_1 = C_N V_1$, $q_1 = C_B V_2$, $q_2 = C_I V_2$ and arrive at $W = C_N V_1^2 (1 - C_I/C_B)\ (C_N/C_B - 1)$. We see that C_B should be chosen between the two extreme values and to maximize output: $C_I C_N /\ C_B = (1/2)(C_I + C_N)$. Defining a capacitance ratio $\xi \equiv C_N/C_I > 1$, we can write the maximum output, $W_m(\xi)$, as

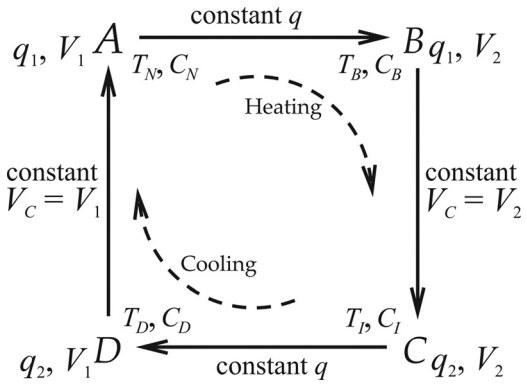

FIG. 2. Operating cycle of proposed charge pump. As temperature rises, capacitance drops, $C_B < C_N$, and since charge is constant, voltage rises to V_2. Further increase in temperature decreases capacitance further, $C_I < C_B$, but charge can now flow out at the higher voltage V_2. Cooling $T_I \rightarrow T_D$ causes the capacitance to rise again, $C_D > C_I$, and the voltage drops to the point where charge can be received from the source at V_1.

$$W_m(\xi) = C_N V_1^2 \frac{(\xi - 1)^2}{4\xi} \tag{1}$$

Thus, given a decrease in capacitance ratio ξ upon heating, we can output $W_m(\xi)$ per cycle, with the optimal intermediate state B chosen by $C_B = 2C_N/(\xi + 1)$, and a corresponding voltage gain $V_2/V_1 = (1/2)(1 + \xi)$. Output is much higher at a higher operating voltage, V_1. It is possible to use self-priming circuits in this context that increase V_1 with each cycle executed.[4]

More important than the output per cycle is rather the output per second (power). For the period of a cycle, τ, a lower limit is the time taken for the necessary heat input, $H_{in}Ad$ for the capacitor material, where H_{in} is the energy per unit volume, and A and d are the material area and thickness. This limit gives $\tau_{\min} = H_{in}d/I_{sun}$, where I_{sun} is the incident solar flux. The incident solar flux ranges from an average of $100\mathrm{W/m^2}$ on average in Britain, to a peak value of $1.4\mathrm{kW/m^2}$ in equatorial deserts.[1] Other time delays include mechanical, heat-diffusive or electrical effects.

If a cycle takes a time τ, the power output per unit area is $W_m(\xi)/(A\tau)$ and the efficiency is therefore $W_m(\xi)/(\tau I_{sun}A)$. This power efficiency is maximized when it limited only by the rate energy is put in, that is when a cycle time is $\tau_{\min}$: the upper limit is then $W_m/(H_{in}Ad)$.

We now turn out attention to materials which would be suitable for the capacitor. A necessary condition is to give a large change in capacitance on heating. For a material of relative dielectric constant ε, the capacitance per unit area is $C/A = \varepsilon\varepsilon_0/d$ which appears throughout above via W_m/A. We identify two possibilities: (a) a temperature dependent dielectric constant, and (b) temperature induced deformation, that is changing A and/or d. We now explore possibility (a) using liquid crystals. Liquid crystal elastomers will offer both possibilities (a) and (b) and further advantages of electrostatic stability.

B. Properties of liquid crystals

Liquid crystals are anisotropic fluids which undergo a thermal phase change at a transition temperature T_{ni} from a nematic to an isotropic phase. They are suitable materials for a charge pump, since a liquid crystal capacitor will have a temperature-dependent dielectric constant. To understand this temperature dependence, a molecular description of the material is required.

Liquid crystals are composed of rodlike molecules which show long range orientational order, as sketched in Fig. 3.

The long molecular axes tend to align with angles θ around a particular direction, specified by the director, $\underline{n}$. For uniaxial nematogens, the appropriate symmetry about the director is quadrupolar with order parameter,

$$Q = \langle P_2(\cos\theta)\rangle = \tfrac{1}{2}\langle 3\cos^2\theta - 1\rangle \tag{2}$$

giving the degree of nematic ordering

The liquid crystal rods have different polarizabilities along and perpendicular to their long molecular axis. Summing

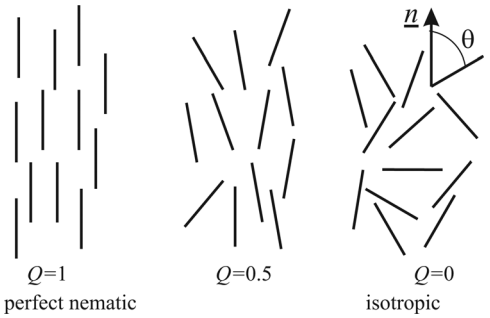

FIG. 3. Distribution of molecular axes around the average alignment direction, $\underline{n}$. Degree of ordering is quantified by the order parameter Q.

over the contributions from all molecules, the dielectric tensor is in its most general form:

$$\underline{\underline{\varepsilon}}(Q) = \bar{\varepsilon}(1-Q)\underline{\underline{\delta}} + Q\left[\varepsilon_{\perp}^{0}\underline{\underline{\delta}} + (\varepsilon_{\parallel}^{0} - \varepsilon_{\perp}^{0})\underline{n}\,\underline{n}^{T}\right] \tag{3}$$

where $\bar{\varepsilon} = \frac{1}{3}(2\varepsilon_{\perp}^{0} + \varepsilon_{\parallel}^{0})$ is the isotropic value; $\varepsilon_{\parallel}^{0}$ and $\varepsilon_{\perp}^{0}$ are the values parallel and perpendicular to the director for the $Q=1$, perfectly nematic phase. The values of the susceptibilities along and perpendicular to the director at intermediate order Q are respectively $(1/3)[(1+2Q)\varepsilon_{\parallel}^{0} + 2(1-Q)\varepsilon_{\perp}^{0}]$ and $(1/3)[(1-Q)\varepsilon_{\parallel}^{0} + (2+Q)\varepsilon_{\perp}^{0}]$. The sign of the intrinsic anisotropy $\Delta\varepsilon^{0} = \varepsilon_{\parallel}^{0} - \varepsilon_{\perp}^{0}$, and the direction of ordering, $\underline{n}$, with respect to the capacitor plates can be chosen such that the capacitance decreases with rising temperature. From Eq. (3) the current anisotropy is then $\Delta\varepsilon = Q\Delta\varepsilon^{0}$.

The temperature dependence of the nematic order, Q derives from the Landau free energy density which, near a characteristic temperature T^{*}, is:

$$F_{nem} = \tfrac{1}{2}a_0(T-T^{*})\,Q^2 - \tfrac{1}{3}bQ^3 + \tfrac{1}{4}cQ^4. \tag{4}$$

When external fields act, for instance electrical or mechanical, they couple in the first approximation like $-fQ$ which subtracts from F_{nem} since on storing energy in the dielectric charge is taken from the battery and overall energy decreases. We discuss below the electrical coupling represented by the f term. It arises from energy densities of the form $(1/2)\Delta\varepsilon\varepsilon_0 E^2$ and hence is linear in Q. The order parameter minimizing $F_{nem} - fQ$ is shown as a function of T in Fig. 4 and determines how the dielectric tensor varies with temperature. The cyclic process generates a net work output when the external field is nonzero, since the heat absorbed in stages A to C is greater than the heat released in stages C to A.

Upon heating, the order parameter follows a different $Q(T)$ curve than on cooling, due to a different applied field (see Fig. 5). It is the subtle differences in the $Q(T)$ path, analogous to the familiar pressure-volume diagrams for ideal gas heat engines, that gives a work output. This observation brings us to the crux of the matter - we need to be operating at fields comparable to the critical field, E_{cp}, in order to generate substantial energy (compared to the energy absorbed in the cycle). E_{cp} is estimated by identifying $f_{cp} \sim (1/2)\varepsilon_{\parallel}^{0}\varepsilon_0 E_{cp}^2$ to give $E_{cp}=2\times10^{8}\mathrm{V/m}$. However liquid crystals cannot operate at such high fields. Ionic impurities can conduct across the liquid crystal as the external field is increased, and

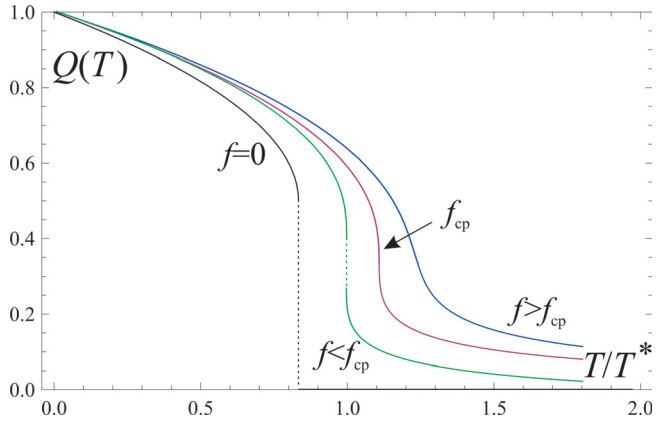

FIG. 4. (Color online) Order parameter vs temperature T generated by minimizing $F_{nem}(Q) - fQ$, where the linear term is the first order effect of an external field. Field strengths f are indicated. Note the discontinuous change in Q at T_{ni} disappears at the critical point, $f_{cp} = b^3/27c^2$ (Ref. 5).

breakdown is reached for a typical field $E_{*} = 3\times10^{7}\mathrm{V/m}$ (Ref. 6).

This limit can be quantified by considering a liquid crystal-filled capacitor. Assume heating reduces the permittivity from $\varepsilon_{\parallel}^{0} = 16$ to $\bar{\varepsilon} = 8$, such that $\xi = 2$. Therefore:

$$W_m = \tfrac{1}{8}C_N V_1^2 = \tfrac{1}{8}\varepsilon_{\parallel}^{0}\varepsilon_0 E_1^2\Omega \tag{5}$$

where $\Omega = Ad$ is the volume of the capacitor

We can roughly estimate the heat input (for $E \ll E_{cp}$) as that which is needed to overcome the nematic liquid crystal interaction and disorder the orientation of the molecules. This is of the order nkT_{NI} per volume, where n is the number density of molecules and T_{NI} is the nematic-isotropic transition temperature. An estimate for the efficiency is then

$$\eta = \frac{\varepsilon_{\parallel}^{0}\varepsilon_0 E_1^2}{8nkT_{NI}} \tag{6}$$

and we see that this is vanishingly small unless the electric energy density is comparable to the energy density of the

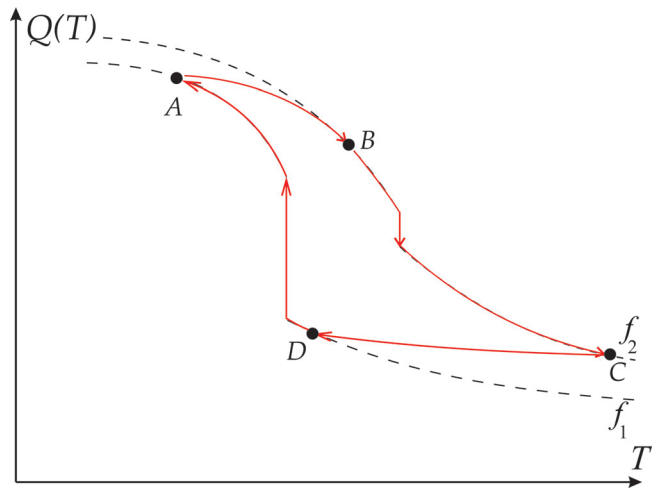

FIG. 5. (Color online) Schematic of a charge pump undergoing the cycle, described in Fig. 2, with reduced external fields f_1 and f_2. Note resemblance to a conventional p-V diagram.

nematic interaction. For an effective charge pump with non-negligible efficiency, we must therefore have

$$\tfrac{1}{2}\Delta\varepsilon\varepsilon_0 E_*^2 \sim nkT_{NI}. \tag{7}$$

Using typical values of $n \sim 10^{27}$ m^{-3} and $\Delta\varepsilon \sim 10$, we obtain $E_* \sim 10^8$V/m which is very large.

This analysis is not specific to liquid crystals and so the requirements of a large field therefore apply to many other systems. To follow the heat flow in and out of the system during the course of a cycle, one must model the energy not simply at constant field $\underline{E}$ (the constant voltage sections BC and DA of Fig. 2), but also at constant $\underline{D}$ (the constant charge sections AB and CD) – we address this elsewhere.

These considerations lead us to consider liquid crystal elastomers, which have a principal advantage - elastomers can operate at much higher fields. An example of dielectric elastomers operating as generators have for instance operating fields of up to 4×10^8V/m.[4]

C. Liquid crystal elastomers

Liquid crystal elastomers (LCEs) are conventional crosslinked polymers, combined with liquid crystalline order of rigid backbone units. We explore the properties which make these materials interesting - specifically contraction on heating. The key point is that the strain is coupled to nematic order, and so the elastic properties of the rubber can be modified with temperature, or even light.[8] These effects arise due to the anisotropy of the polymer backbone.

A classical polymer is composed of a network of chains, and the chains are assumed to be rigid over a length scale a. A single chain of N units traces a random walk of fixed step length a. If we take the end-to-end vector of a single chain, $\underline{R}$, we can express the expected lengths as $\langle R_i R_j\rangle = (1/3)\ell_{ij}\mathcal{L}$, where $\mathcal{L} = Na$ is the fully stretched chain length. For rubbers, $\underline{\underline{\ell}}$ is isotropic, but for nematic elastomers $\underline{\underline{\ell}}(Q)$ has an anisotropic form $\underline{\underline{\ell}} = \ell_\perp\underline{\underline{\delta}} + (\ell_\parallel - \ell_\perp)\underline{\mathrm{n}}\,\underline{\mathrm{n}}^T$, with $\underline{\mathrm{n}}$ again the director. The simplest model for $\underline{\underline{\ell}}(Q)$ is the freely jointed chain model, where the isotropic step lengths are a and the anisotropic step lengths are:

$$\ell_\perp(Q) = a(1-Q), \quad \ell_\parallel(Q) = a(1+2Q). \tag{8}$$

The elastic properties of the material are largely determined by the polymer network. In classical rubbers, the network deforms via low energy conformation changes and hence the free energy of the system is dominated by entropy. We can consider each chain to perform a random walk in 3D, with a Gaussian probability distribution for a total span R:

$$p(R^2) = \frac{1}{\mathcal{N}}\exp\left[-\frac{3R^2}{2a\mathcal{L}}\right] \tag{9}$$

where $\mathcal{N}$ is a normalization. We can consider deforming the rubber $\underline{\tilde{\mathrm{R}}} = \underline{\underline{\lambda}}\cdot\underline{\mathrm{R}}$ where $\underline{\underline{\lambda}}$ is the deformation gradient tensor. We then form the partition function $Z \propto p(\tilde{R}^2)$ and the free energy density, $\mathrm{F} = -kT\langle \ln Z\rangle_R$, by averaging overall chains in the network, giving:

$$F = \tfrac{1}{2}n_s kT\mathrm{Tr}\left[\underline{\underline{\lambda}}^T\cdot\underline{\underline{\lambda}}\right] \tag{10}$$

where n_s is the cross-link density (that is, related to the number density of such strands), and the elastic shear modulus can be identified as $\mu = n_s kT$. The normalization adds a constant to the free energy which can be ignored. Furthermore, rubber deforms at constant volume, $\mathrm{Det}(\underline{\underline{\lambda}}) = 1$, since the bulk modulus greatly exceeds the shear modulus. This constraint contributes to the highly nonlinear elasticity of rubbers.

Similar reasoning can be applied to nematic elastomers,[5] but with an anisotropy introduced via a Gaussian with an anisotropic second moment tensor $\langle R_i R_j\rangle = (1/3)\ell_{ij}\mathcal{L}$. In deforming from a relaxed state $\underline{\underline{\ell}}^0$ to a new state characterized by $\underline{\underline{\ell}}$ and $\underline{\underline{\lambda}}$, the free energy is written:

$$F_{el} = \tfrac{1}{2}\mu\mathrm{Tr}\left[\underline{\underline{\ell}}^0\cdot\underline{\underline{\lambda}}^T\cdot\underline{\underline{\ell}}^{-1}\cdot\underline{\underline{\lambda}}\right] + \mathrm{const}(Q) \tag{11}$$

where the additional Q-dependent term comes from the modified normalization. It is independent of the deformation $\underline{\underline{\lambda}}$ and simply adds to the Q^n terms in the Landau free energy, Eq. (4). We henceforth ignore it.

Figure 6 shows spontaneous strains, λ_m, which experimentally can be up to 500%, and are described by Eq. (11) which gives $\lambda_m = \left(\ell_\parallel/l_0\right)^{1/3}$. Another advantage of using nematic rubbers as the capacitor material is that the changing dielectric anisotropy due to the changing order of the component rods gives an even larger change in capacitance upon heating, as discussed in Sec. II B.

Koh *et al.*[9] have investigated the mechanical energy involved in a cycle of expanding and contracting dielectric elastomer. They estimate a maximal possible energy density per cycle of $6.3\mathrm{J/g} \sim 6 \times 10^6\mathrm{Jm}^{-3}$ (using density $\rho = 1000\mathrm{kg\,m}^{-3}$).

D. Input energy

A final point to consider is the input solar energy required to make the transition from the nematic to the isotropic phase.

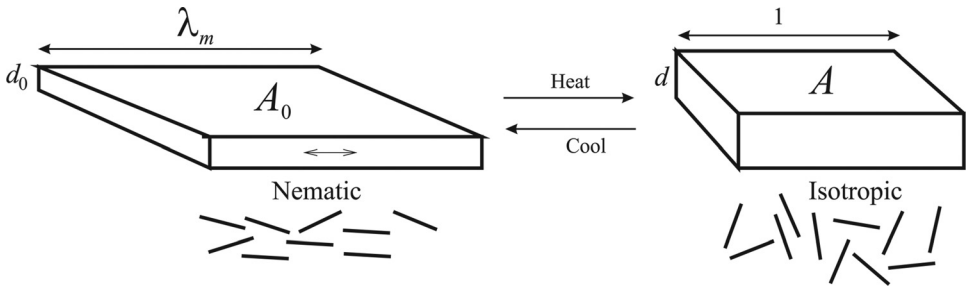

FIG. 6. Decrease of capacitance upon heating, with $d = d_0\lambda$ and $A = A_0/\lambda$. $C \propto A/\mathrm{d}$ so $\xi \propto \lambda^2$ for a constant volume deformation.

For liquid crystals, a lower bound is the latent heat, which takes a value $L = (1/2)A_0 Q_{ni}^2 T_{ni} = 2 \times 10^6 \mathrm{Jm}^{-3}$(Ref. 5). When specific heats are accounted for, we arrive at an estimate $H_{in} = 3 \times 10^6 \mathrm{Jm}^{-3}$ for an order parameter change of $Q_A = 0.5$ to $Q_C = 0$. It is difficult to compute an exact value of input energy for the charge pump, since the degree of ordering in a nematic elastomer depends on a number of complex factors:

(1) the network cross-linking
(2) the coupling coefficient of strain to nematic order
(3) the effect of the external field

For example, Disch *et al*. have found that cross-linking and imposed strains result in a $Q(T)$ dependence markedly different from the conventional liquid crystal case.[10] In particular, the transition appears supercritical - the loss of a first order phase transition.[11]

Recent developments in azo dyes have sparked interest in optically induced order changes and highlight the possibility of using light to capture solar energy. However[12] suggest the required solar input to be $H_{light} \sim 10^7 \mathrm{J/m}^3$. The energy is high because although few rods need to absorb a photon to bend and thus, destroy the nematic order, each photon carries energy far in excess of the thermal energies required to disorder the nematic phase by temperature rise alone. Since these energies exceed those of heat input, we shall not pursue optical effects here. However, dye molecules would aid the absorption of heat in the form of light, and would contribute to the decline of the nematic state, that is they would be still valuable.

We must also consider the cooling stages of the cycle and can offer several ways of shielding the capacitor from the incident solar energy. A reflective electrochromic layer could be activated at an appropriate point in the cycle, which would allow heat to diffuse out of the capacitor. Alternatively, an array of capacitors could be sequentially illuminated and then allowed to cool, either via a movable focusing mirror, or by mounting the array of capacitors on a rotating system. Issues surrounding the cooling phase are further explored in the discussion section.

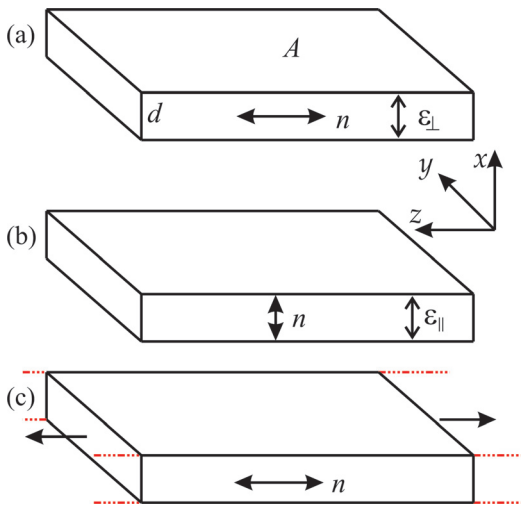

FIG. 7. (Color online) In each case, a capacitor with a LCE as the working substance - flexible electrodes are attached directly to the sample surfaces. The three proposed geometries: (a) director in plane, (b) director along x direction and (c) director in plane, with prestretch. The separation is $d = d_0\lambda$ where d_0 is the unstrained dimension. The volume, $\Omega = Ad$ is conserved.

III. MODELING THE ELASTOMERIC CHARGE PUMP

We proceed to model the proposed charge pump using a liquid crystal elastomer cyclically and reversibly. The aim is to compute the electrical power output of the pump. Referring to Fig. 7, the capacitance of this system can be written:

$$C = \frac{\varepsilon\varepsilon_0 A}{d} = \frac{\varepsilon\varepsilon_0 \Omega}{d_0^2}\lambda^{-2} \tag{12}$$

where ε is the xx-component of $\underline{\underline{\varepsilon}}$. It is $\varepsilon_\parallel$ or $\varepsilon_\perp$, depending on the geometry chosen. On heating from the nematic to the isotropic phase, we wish the capacitance to decrease, which is achieved by changes in λ, i.e., in the geometry of the capacitor, and by changes in ε.

A. Choice of geometry

We consider three geometries:

(a) The elastomer has $\underline{\mathrm{n}}$ in plane and contracts along the z direction upon heating to the isotropic phase. Choose $\varepsilon_\perp^0 > \varepsilon_\parallel^0$ so that $\varepsilon_\perp$ decreases on heating. The relative change in capacitance upon heating is limited by $\varepsilon_\perp/\bar{\varepsilon} = 3/(2 + (\varepsilon_\parallel^0/\varepsilon_\perp^0))$ which has a maximum 3/2.
(b) The elastomer has $\underline{\mathrm{n}}$ normal to the plane. Choose $\varepsilon_\parallel^0 > \varepsilon_\perp^0$ to ensure a decrease in capacitance on heating. An upper limit on the relative capacitance change is now 3 since $\varepsilon_\parallel^0/\bar{\varepsilon} = 3/\left[1 + 2(\varepsilon_\perp^0/\varepsilon_\parallel^0)\right]$. We do not want the nematic contraction to counteract this effect, so we choose $\ell_\parallel^0 \approx \ell_\perp^0$ (or ideally $\ell_\parallel^0 < \ell_\perp^0$, an oblate phase, so that heating also makes the sample fatter).
(c) Corbett *et al*. have shown that imposing a fixed strain in one direction can increase the mechanical efficiency of electro-actuation in LC elastomers,[13] as is known for conventional dielectric elastomers.[9,14] We will explore this scenario in our model, with a prestrain λ_0 in the y direction, for $\underline{\mathrm{n}}$ along z.

B. Calculation of output work

For each proposed geometry, the capacitor undergoes a cyclic change, as described in Fig. 2 and Sec. II A. As shown in deriving Eq. (1), the maximum work output, $W_m(\xi)$, depends only on the high and low capacitance values in the cycle, not the intermediate path taken. We therefore need only model the nodes A and C in the cycle Fig. 2 to obtain the optimal output.

The capacitance at node A may be calculated either via a constant charge calculation from A to B, or via a constant voltage calculation from D to A. For a self-consistent cycle, the two results are equal. We will use constant voltage calculations, since we are interested in the operating voltages, V_1 and V_2, and factors which constrain them, rather than the capacitor charges q_1 and q_2.

For the system in equilibrium at constant voltage, we write the free energy per unit volume as:

$$F(Q,\lambda) = F_{nem}(Q) + F_{el}(Q,\lambda) - C(Q,\lambda)V^2/2\Omega \quad (13)$$

with F_{nem} from Eq. (5), with the external field coupling $-fQ$ now specified through the capacitor energy, and F_{el} from Eq. (12) with $\underline{\underline{\ell}} = \underline{\underline{\ell}}(Q)$. The energy F (Q, λ) is minimized with the added complication that the diodes prevent backflow of charge. This constrains the sign of the capacitance change such that C is decreasing along B to C, and increasing along A to D. The minimization of $F(Q, \lambda)$ is subject to constraints—a difficult problem.

To make analytical progress, we can decouple Eq. (13) into separate strain-dependent and Q-dependent components. The coefficients a_0, b, c in Eq. (5) are of the order nkT, where n is the number density of nematogens; while $\mu \sim n_s kT$, where n_s is the number density of crosslinks. We expect $n \sim (10-100)\, n_s$, so that F_{nem} and F_{el} can be separated. Under the further assumption that the electric field across the capacitor, E, is significantly less than the the critical field, E_{cp}, the final term of Eq. (14) can also be separated from F_{nem}. This is only an approximation, and we later find that E/E_{cp} has a typical value of 10%. If we accept this approximation, the equilibrium order parameter, Q_* is determined by minimizing $F_{nem}(Q)$. The equilibrium strain is then found by minimizing $F_{el}(\lambda) - C(\lambda)V^2/2\Omega$ at the fixed parameter Q_*. This simplification permits an analysis of the problem, but introduces inaccuracies into the model.

Finally, we use this machinery to calculate the equilibrium strains for the low and high limits, λ_A and λ_C. Having found these, we can compute the capacitance ratio $\xi = C_N/C_I = \varepsilon_A\lambda_C^2/\varepsilon_C\lambda_A^2$, and subsequently the electrical output of the device, Eq. (1).

C. Case (a): director in plane

Consider geometry (a) described in Fig. 7. The strain-dependent free energy is found by decoupling Eq. (13). Using $\underline{\underline{\ell}} = \mathrm{diag}(\ell_\perp, \ell_\perp, \ell_\parallel)$ and the constraint of constant volume, $\mathrm{Det}(\underline{\underline{\lambda}}) = 1$, we arrive at

$$F(\lambda, \lambda_{zz}) = \tfrac{1}{2}\mu\left[\frac{\ell_\perp^0}{\ell_\perp}\left(\lambda^2 + \lambda^{-2}\lambda_{zz}^{-2}\right) + \frac{\ell_\parallel^0}{\ell_\parallel}\lambda_{zz}^2\right] - \frac{\varepsilon_\perp\varepsilon_0 V^2}{2d_0^2\lambda^2}. \quad (14)$$

Defining the step length ratios $p_\perp(Q) = \ell_\perp^0/\ell_\perp$, $p_\parallel(Q) = \ell_\parallel^0/\ell_\parallel$ and characteristic ratio $V_m^2 = \mu d_0^2/\varepsilon_0$, and minimizing over λ_{zz}, we obtain:

$$F(\lambda) = \tfrac{1}{2}\mu\left[p_\perp\lambda^2 + 2\frac{\sqrt{p_\perp p_\parallel}}{\lambda} - \varepsilon_\perp\left(\frac{V}{V_m}\right)^2\lambda^{-2}\right]. \quad (15)$$

V_m is the voltage where the strain energy is comparable to the stored elastic energy. We assume nematic network genesis, so that at the point A in the cycle $p_\perp = p_\parallel = 1$ and $\varepsilon_\perp = \varepsilon_A$ since Q is at the value it took at network formation. To find the equilibrium strain at A, we must then minimize the free energy with constant V fixed at its initial value V_1:

$$F_1(\lambda) = \tfrac{1}{2}\mu\left[\lambda^2 + 2\lambda^{-1} - \varepsilon_A(V_1/V_m)^2\lambda^{-2}\right] \quad (16)$$

with the additional condition that λ must be decreasing. It is simplest to solve the quartic equation $\partial F_1/\partial\lambda = 0$ to find the minimum energy. We must confirm *post hoc* that λ decreases along D to A, to a minimum value λ_A at A, as expected due to nematic contraction along z on cooling.

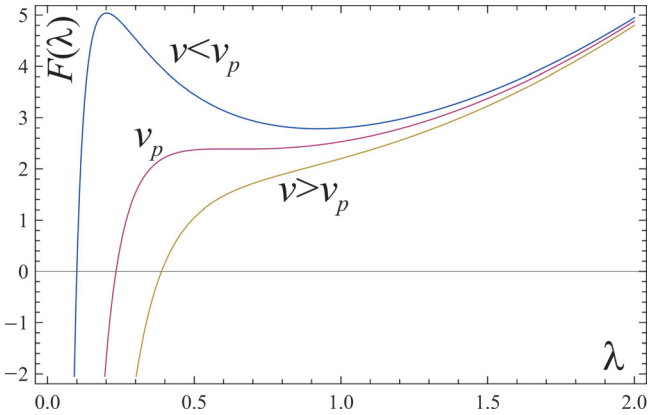

FIG. 8. (Color online) The free energy $F_1(\lambda)$ for various reduced working voltages, v. For $v < v_p$, there is a clear minimum in free energy, disappearing for $v > v_p$, the lower plot. The limiting case, when the two extrema coincide, has $F_1^{(1)}(\lambda_p) = F_1^{(2)}(\lambda_p) = 0$, which yields for rubber $v_p = 3/4^{4/3}$ (Ref. 16).

Díaz *et al.*[15] identified an upper limit on the operating voltage, V_1. Define a reduced (squared) form of V_1, the operating voltage: $v \equiv \varepsilon_A V_1^2/V_m^2$. For $v > v_p$, with v_p characteristic of a material, there is no local minimum in free energy. For instance, for a classical rubber $v_p = 3/4^{4/3}$. Charge flows onto the capacitor and the rubber is compressed further and further, leading to so called 'pull-in' runaway, as illustrated in Fig. 8.

Upon heating to the isotropic phase, the order parameter is reduced and the capacitance of the system decreases. The free energy at C may be written:

$$F_2(\lambda) = \tfrac{1}{2}\mu\left[p_\perp\lambda^2 + 2\frac{\sqrt{p_\perp p_\parallel}}{\lambda} - \left(\frac{\varepsilon_C V_2^2}{\varepsilon_A V_1^2}\right)a\lambda^{-2}\right] \quad (17)$$

with $p_\perp = \ell_\perp^0/\bar{l} < 1$, $p_\parallel = \ell_\parallel^0/\bar{l} > 1$, estimated using the freely jointed chain model. We take the state C to be approximately isotropic, that is the fields do not induced appreciable order, and hence it is $\bar{l}$ that enters the ps. The energy $F_2(\lambda)$ must be minimized with the diode constraint - that λ must increase - which means pull-in is avoided at V_2. Recalling $\xi = \varepsilon_A\lambda_C^2/\varepsilon_C\lambda_A^2$ and that $V_2/V_1 = \frac{1}{2}(\xi+1)$, we can minimize Eq. (17) to give the strains and capacitance ratio $\xi(v)$. From there, we can obtain the optimal work output as a function of the operating voltage:

$$W_m = \frac{(\xi-1)^2}{4\xi}C_N V_1^2 = \frac{(\xi-1)^2 v}{4\xi\lambda_A^2}\mu\Omega, \quad (18)$$

see Fig. 9.

We model the case for v below a critical value, v^* such that λ decreases along D to A, and increases along B to C (which is verified *post hoc*). We find that W is maximal for $0 < v < v^*$, so only need model this case.

To determine v^*, we find that the solution of $\partial F_2/\partial\lambda = 0$ gives λ decreasing along B to C, unless the pull-in limit is reached somewhere along B to C - where there is no local minimum in $F_2(\lambda)$. This first occurs when $F_2'(\lambda_p) = F_2''(\lambda_p) = 0$ at C; these two conditions are solved simultaneously to give:

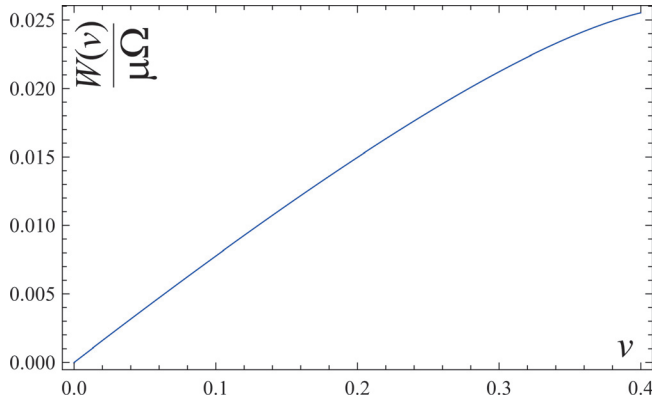

FIG. 9. (Color online) The reduced maximum work $W_m(v)/\mu\Omega$ against reduced operating voltage v less than the critical value v^*, case (a).

$$v^* = \frac{\varepsilon_A}{\varepsilon_C}\left(\frac{2}{\xi+1}\right)^2 \frac{3}{4^{4/3}} p_\perp \left(\frac{p_\parallel}{p_\perp}\right)^{2/3}. \tag{19}$$

Figure 9 assumes the order parameter changes from $Q_A = 0.5$ to $Q_C = 0.02$. This has been observed in elastomers by Disch *et al.*[10] over a temperature range of 50K. The dielectric constants are $\varepsilon_A = \bar{\varepsilon} + (\varepsilon_\perp^0 - \bar{\varepsilon})Q_A$ and $\varepsilon_C = \bar{\varepsilon}$. There are many material values to choose from. We use data from[17] which are: $\varepsilon_\perp^0 = 20$, $\varepsilon_\parallel^0 = 10$. We assume the step lengths are given by the freely jointed chain model, Eq. (8): $p_\parallel = (1+2Q_A)/(1+2Q)$, $p_\perp = (1-Q_A)/(1-Q)$ (Ref. 5).

For the chosen parameters the maximal work output is obtained at $v = v^* = 0.4$. Using $\mu \approx 10^6$,[5] and a $d_0 = 50\mu$m thick capacitor, we find that the optimal output per unit volume is $W_m/\Omega = 2.5 \times 10^4 \mathrm{Jm}^{-3}$ operating at a voltage $V_1 = 2.5$kV and $V_2 = 3.1$kV.

D. Case (b): Director along *x* direction

The method of the previous section can be also used to characterize the charge pump of Fig. 7(b). The director is now taken along the slab normal, $\underline{x}$, so $\underline{\underline{\ell}} = \mathrm{diag}(\ell_\parallel, \ell_\perp, \ell_\perp)$. The free energy at A is now written:

$$F(\lambda, \lambda_{zz}) = \tfrac{1}{2}\mu\left[p_\perp\left(\lambda_{zz}^2 + \frac{1}{\lambda^2\lambda_{zz}^2}\right) + p_\parallel\lambda^2 - \frac{\varepsilon_\parallel}{\varepsilon_\perp}\frac{v}{\lambda^2}\right]. \tag{20}$$

The same procedure is followed, but assuming (a) $\ell_\parallel^0 \approx \ell_\perp^0$ such that the nematic elastomer contraction is negligible and (b) $\varepsilon_\parallel^0 > \varepsilon_\perp^0$ and the dielectric constants are similar to the data described by Schadt[7]: $\varepsilon_\parallel^0 = 16$, $\varepsilon_\perp^0 = 4$. We obtain a maximal output of $W_m/\Omega = 2.5 \times 10^4 \mathrm{Jm}^{-3}$ operating at a voltage $V_1 = 3.1$kV and $V_2 = 3.8$kV.

E. Case (c): Director in plane, with prestretch imposed

We model how a fixed prestrain λ_0 can enhance the electrical output of the charge pump described by Fig. 7(c). We shall use the same material properties as given in case (a). In a familiar notation, we construct the free energy density of the system at points A and C:

$$F_1(\lambda) = \tfrac{1}{2}\mu\left[\lambda^2 + \lambda_0^2 + \lambda_0^{-2}\lambda^{-2} - v/\lambda^2\right] \tag{21}$$

$$F_2(\lambda) = \tfrac{1}{2}\mu\left[p_\perp\lambda^2 + p_\perp\lambda_0^2 + \frac{p_\parallel}{\lambda^2\lambda_0^2} - \frac{\varepsilon_C V_2^2}{\varepsilon_A V_1^2}\frac{v}{\lambda^2}\right]. \tag{22}$$

In the spirit of the previous section, we minimize the free energies with an additional constraint on the sense in which λ changes. As before, solve $\partial F_1/\partial\lambda|_A = \partial F_2/\partial\lambda|_C = 0$ and verify that λ is changing in the correct sense. Using $\xi = \varepsilon_A\lambda_C^2/\varepsilon_C\lambda_A^2$ and $V_2/V_1 = (1/2)(\xi+1)$ we obtain an implicit equation for ξ:

$$\xi^2 = \left(\frac{\varepsilon_A}{\varepsilon_C}\right)^2 \frac{p_\parallel\lambda_0^{-2} - \left(\frac{1}{4}\varepsilon_C\varepsilon_A^{-1}v\right)(\xi+1)^2}{p_\perp\left(\lambda_0^{-2} - v\right)}. \tag{23}$$

Plots of the work output show it monotonically increases with reduced working voltage, v, for a given λ_0. However, Corbett *et al.*[13] highlight a constraint that prestraining raises, namely upper limits on V_1 and V_2: At high fields, the Maxwell stress causes a compression in the x direction. The elastomer is liable to expand in the z and y directions. Above a certain voltage, the tension holding the prestrain λ_0 becomes a compression and the sheet will wrinkle. This critical point is given where the stress in the y direction, $\sigma_{yy} = \partial F/\partial\lambda_{yy}$, is zero. If we use the additional condition for equilibrium, $\partial F/\partial\lambda = 0$ we obtain wrinkling voltages at A and C:

$$v_w^{(1)} = \lambda_0^{-2} - \lambda_0^{-8} \tag{24}$$

$$v_w^{(2)} = \frac{\varepsilon_A V_1^2}{\varepsilon_C V_2^2} p_\parallel\left[\lambda_0^{-2} - \left(p_\parallel/p_\perp\right)\lambda_0^{-8}\right], \tag{25}$$

see Fig. 10. The second condition is complicated, since the two voltages are related via ξ which itself is a function of the prestrain. To understand the constraint, we shall let $\xi \approx 2$ to estimate the wrinkling limit.

We note that the work output monotonically increased with v for a given prestrain. Consequently, in order to maximize output we operate at, or very close to, the wrinkling value. This output, as a function of the prestrain, is plotted in Fig. 11. The maximum output is approached for strains above $\lambda_o \approx 1.5$ and is $W_m/\Omega = 1.1 \times 10^5 \mathrm{Jm}^{-3}$ per cycle.

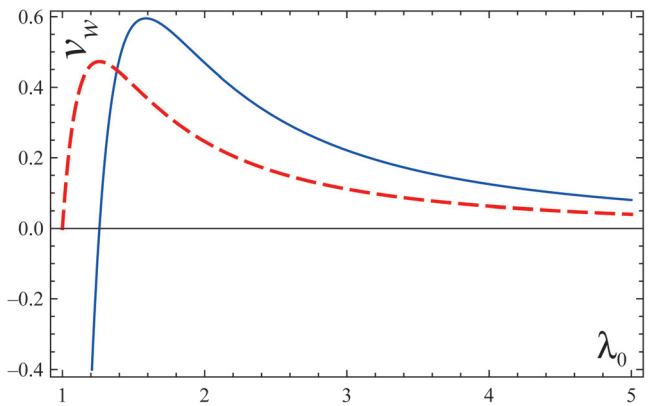

FIG. 10. (Color online) Plots of the two reduced wrinkling voltages as functions of prestrain. For $\lambda_o > 1.38$ we see that $v_w^{(1)}$ (solid blue) is most appropriate. For $\lambda_0 < 1.25 = \left(p_\parallel/p_\perp\right)^{1/6}$ the wrinkling voltage, $v_w^{(2)}$ (heavy dashed red), is zero. This is because the sample will tend to contract along z, hence, expand along y upon heating.

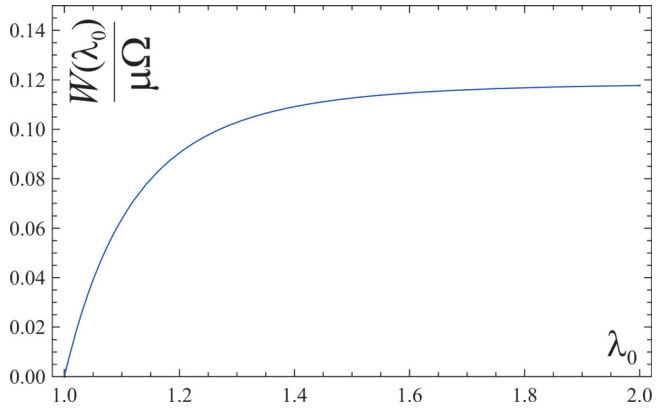

FIG. 11. (Color online) Optimal output, $W_m/\mu\Omega$, as a function of prestrain, λ_0, and valid for $\lambda_0 > 1.38$ when $v_w^{(1)}$ is used.

For a $d_0 = 50\ \mu$m thick capacitor, the operating voltages are $V_1 = 2.7$kV and $V_2 = 3.8$kV.

IV. CONCLUSIONS

We have computed the maximum electrical output of the charge pump. We modeled the elastic and dielectric properties of nematic elastomers for several geometries and optimized the output in each case. Remembering an upper efficiency bound of $W_m/H_{in}\Omega$, we generate the results:

(1) director in plane, $\eta = 0.025\mu/H_{in} \approx 1\%$
(2) director along x, $\eta = 0.025\mu/H_{in} \approx 1\%$
(3) prestretch along y, $\eta = 0.11\mu/H_{in} \approx 4\%$

Our predominant approximation was to decouple strain from nematic order, and in particular how this affects the heat needed to change the order parameter. In reality, the input heat should be a function of both strain and stiffness, μ. It is known that mechanical stress little effects the magnitude of order. Further, we have taken $\mu = 10^6\text{Jm}^{-3}$, which may be too high in practice. For highly crosslinked elastomers, the network becomes increasingly stiff and the effect of nematic contraction greatly diminishes.

Secondly, realistic limits on the prestrain λ_0 must be examined. The proposed strain of 1.5 is not unusual; a less conservative estimate would increase the efficiency.

We must also consider what limits the time period for a single cycle of the pump. The obvious factor is the time taken to absorb the required energy, $\tau_1 = H_{in}d_0/I_{sun}$. We will consider I_{sun} to be the atypical average for Britain — 100W/m^2.[1] We take $d_0 = 50\ \mu$m.

Heat transfer is also limited by diffusion. We can envisage absorbing the heat via dye molecules embedded in the elastomer, which would be relatively fast. However, there would be a time $\tau_2 \sim d_0^2/D$ for heat to diffuse out in the cooling stages. (D, the diffusion coefficient, was measured for these types of elastomers to be $D = 1.5 \times 10^{-7}\text{m}^2/\text{s}$ by Hon *et al.*[18]). Thus, τ_2 becomes comparable to τ_1 when $d_0 \approx DH_{in}/I_{sun} \approx 5$mm. For a 50 μm thick capacitor we can therefore expect the diffusion effects to be minimal. Furthermore if energy is delivered in the form of light, which is then converted into heat by being absorbed by dye, then no diffusive step is in any case required. Response can be fast – in the tens of milli-second regime,[12] or less. Inertia, see below, would need to be considered.

Other effects include the time for the rubber to deform, of typical magnitude $\tau_3 \sim L_{rubber}/v$, where L_{rubber} is a length scale of the rubber, and the rubber wave speed is estimated as $v = \sqrt{\mu/\rho} \sim 20\ \text{ms}^{-1}$. This is negligible for $L_{rubber} < H_{in}d_0v/I_{sun} \approx 45$ m. The electrical time is also unlikely to be the limiting factor, since it is of order RC, which is often relatively small.

Further considerations concern the large operating voltages ($\sim$ kV) required. At such high voltages, nonideal circuit elements will become important, most notably the diodes at large reverse bias. In addition, the rubber may begin to conduct via charged impurities, which may lead to a significant energy dissipation.

Producing these high voltages may also be a problem. One option is to use electronic DC amplifiers - a 'step up' inserted after the source battery V_1, and a 'step down' inserted before the output battery V_2, as in Fig. 1.

Other potential pitfalls include dealing with a contracting and expanding elastomer, and its fatigue over time; and choosing transparent electrodes (such as grease) to ensure energy is absorbed primarily by the rubber.

While not strictly within the domain of this paper, we end this discussion with a take on the economic viability of the design. An average of 10Wm^{-2} can be produced on rooftops in Britain, but how much will this cost? Photovoltaics currently cost $\sim \$40/\text{W}$ to produce. Given manufacturing data for liquid crystals used in LCD displays, which cost \$5/g, we can roughly estimate an expected cost of raw materials as $\$25/\text{W}$. Again, this seems promising, but we stress that this cost is likely to be a lower estimate. An important extension of this work would be to analyze the efficiencies of polydomain LCE charge pumps. Polydomain materials have the considerable advantage of being much easier to manufacture. Polydomain elastomers, depending on whether they are of isotropic or nematic genesis, can respond to prestress and to electric fields by shape changes at almost zero energy cost[19] by director lamination and evolution of micro-textures.[20,21] Such response offers even greater richness than we report here.

We gratefully acknowledge the financial support of the Cavendish Laboratory (Hiscock), the EPSRC (Warner) and the NSF (Palffy-Muhoray), and valuable discussions with D. Corbett and A. Jakli.

[1] D. J. Mackay, *Sustainable Energy - Without the Hot Air* (UIT, Cambridge, UK, 2009).
[2] M. Green, K. Emery, D. King, Y. Hishikawa, and W. Warta, Prog. Photovoltaics **15**, 35 (2007).
[3] G. Johnson, Natl. Geogr. **216**, 28 (2009).
[4] T. G. McKay, B. O'Brien, E. Calius, and I. Anderson, Smart Mater. Struct. **19**, 055025 (2010).
[5] M. Warner and E. M. Terentjev, *Liquid Crystal Elastomers* (OUP, Oxford, 2007).
[6] I. Dierking, J. Phys. D: Appl. Phys. **34**, 806 (2001).
[7] M. Schadt, J. Chem. Phys. **56**, 1494 (1972).
[8] D. Corbett and M. Warner, Liq. Cryst. **36**, 1263 (2010).
[9] S. Koh, X. Zhao, and Z. Suo, Appl. Phys. Lett. **94**, 262902 (2009).
[10] S. Disch, C. Schmidt, and H. Finkelmann, Macromol. Rap. Commun. **15**, 303 (1994).

[11]A. Tajbakhsh and E. Terentjev, Eur. Phys. J. E **6**, 181 (2001).
[12]M. Camacho-Lopez, H. Finkelmann, P. Palffy-Muhoray, and M. Shelley, Nature Mater. **3**, 307 (2004).
[13]D. Corbett and M. Warner, J. Phys. D **42**, 5 (2009).
[14]G. Kofod, J. Phys. D: Appl. Phys. **41**, 215405 (2008).
[15]R. Díaz-Calleja, E. Riande, and M. Sanchis, Appl. Phys. Lett. **93**, 101902 (2008).
[16]D. Corbett and M. Warner, Sens. Actuators. A **149**, 120 (2009).
[17]D. A. Dunmur, A. Fukuda, and G. Luckhurst, *Physical Properties of Liquid Crystals: Nematics* (Institution of Electrical Engineers, London, 2001).
[18]K. K. Hon, D. Corbett, and E. M. Terentjev, Eur. Phys. J. E **25**, 83 (2008).
[19]K. Urayama, E. Kohmon, M. Kojima, and T. Takigawa, Macromolecules **42**, 4084 (2009).
[20]N. Uchida, Phys. Rev. E **62**, 5119 (2000).
[21]J. S. Biggins, M. Warner, and K. Bhattacharya, Phys. Rev. Lett. **103**, 037802 (2009).